



**HAL**  
open science

## Exercise-induced B-lines in heart failure with preserved ejection fraction occur along with diastolic function worsening

Dejan Simonovic, Stefano Coiro, Marina Deljanin-ilic, Masatake Kobayashi, Erberto Carluccio, Nicolas Girerd, Giuseppe Ambrosio

### ► To cite this version:

Dejan Simonovic, Stefano Coiro, Marina Deljanin-ilic, Masatake Kobayashi, Erberto Carluccio, et al.. Exercise-induced B-lines in heart failure with preserved ejection fraction occur along with diastolic function worsening. *ESC Heart Failure*, 2021, 8 (6), pp.5068-5080. 10.1002/ehf2.13575 . hal-03690638

**HAL Id: hal-03690638**

**<https://hal.univ-lorraine.fr/hal-03690638>**

Submitted on 8 Jun 2022

**HAL** is a multi-disciplinary open access archive for the deposit and dissemination of scientific research documents, whether they are published or not. The documents may come from teaching and research institutions in France or abroad, or from public or private research centers.

L'archive ouverte pluridisciplinaire **HAL**, est destinée au dépôt et à la diffusion de documents scientifiques de niveau recherche, publiés ou non, émanant des établissements d'enseignement et de recherche français ou étrangers, des laboratoires publics ou privés.



Distributed under a Creative Commons Attribution - NonCommercial - NoDerivatives 4.0 International License

# Exercise-induced B-lines in heart failure with preserved ejection fraction occur along with diastolic function worsening

Dejan Simonovic<sup>1†</sup>, Stefano Coiro<sup>2,3†</sup>, Marina Deljanin-Ilic<sup>1</sup>, Masatake Kobayashi<sup>3,4</sup>, Erberto Carluccio<sup>5</sup>, Nicolas Girerd<sup>3,4</sup> and Giuseppe Ambrosio<sup>5,6\*</sup>

<sup>1</sup>Institute for Treatment and Rehabilitation 'Niška Banja', Clinic of Cardiology, University of Niš School of Medicine, Niš, Serbia; <sup>2</sup>Cardiology Department, Santa Maria della Misericordia Hospital, Perugia, Italy; <sup>3</sup>Université de Lorraine, INSERM, Centre d'Investigations Cliniques Plurithématique, INSERM 1433, CHRU de Nancy, Institut Lorrain du Cœur et des Vaisseaux, Nancy, France; <sup>4</sup>INI-CRCT (Cardiovascular and Renal Clinical Trialists) F-CRIN Network, Nancy, France; <sup>5</sup>Division of Cardiology, University of Perugia School of Medicine, Perugia, Italy; and <sup>6</sup>CERICLET—Centro Ricerca Clinica e Traslationale, University of Perugia School of Medicine, Perugia, Italy

## Abstract

**Aims** Pulmonary congestion during exercise assessed by lung ultrasound predicts negative outcome in patients with heart failure with preserved ejection fraction (HFpEF). We aimed at assessing predictors of exercise-induced pulmonary B-lines in HFpEF patients.

**Methods and results** Eighty-one I–II NYHA class HFpEF patients (65.0 ± 8.2 y/o, 56.8% females) underwent standard and strain echocardiography, lung ultrasound, and natriuretic peptide assessment during supine exercise echocardiography (baseline and peak exercise). Peak values and their changes were compared in subgroups according to exercise lung congestion grading (peak B-lines >10 or ≤10). Exercise elicited significant changes for all echocardiographic parameters in both subgroups [39/81 (48.1%) with peak B-lines >10; 42/81 (51.9%) with B-lines ≤10]. Peak values and changes of E-wave (and its derived indices) were significantly higher in patients with >10 peak B-lines compared with those with ≤10 B-line (all *P*-values <0.03), showing significant correlation with peak B-lines for all parameters; concomitantly, global longitudinal strain (GLS) and global strain rate (GSR) during systole (GSRs), early (GSR<sub>e</sub>) and late (GSR<sub>a</sub>) diastole, and isovolumic relaxation (GSR<sub>ivr</sub>) were reduced in patients with B-lines >10 (all *P*-values <0.05), showing a negative correlation with peak B-lines. By adjusted linear regression analysis, peak and change diastolic parameters (E-wave, E/e', GSR<sub>ivr</sub>, and E/GSR<sub>ivr</sub>) and peak GLS were individually significantly associated with peak B-lines. By covariate-adjusted multivariable model, E/e' and GSR<sub>a</sub> at peak exercise were retained as independent predictors of peak B-lines, with substantial goodness of fit of model (adjusted *R*<sup>2</sup> 0.776).

**Conclusions** In HFpEF, development of pulmonary congestion upon exercise is mostly concomitant with exercise-induced worsening of diastolic function.

**Keywords** Heart failure with preserved ejection fraction; Pulmonary congestion; B-lines; Echocardiographic predictors

Received: 24 June 2021; Revised: 19 July 2021; Accepted: 4 August 2021

\*Correspondence to: Prof. Giuseppe Ambrosio, Division of Cardiology, University of Perugia School of Medicine, Ospedale S. Maria della Misericordia, Via S. Andrea delle Fratte, 06156 Perugia, Italy. Tel: +39 0755271509; Fax: 755271244. Email: giuseppe.ambrosio@ospedale.perugia.it

†Dejan Simonovic and Stefano Coiro contributed equally as first authors.

## Introduction

Dyspnoea on exertion is the cardinal symptom reported by patients with heart failure (HF) with preserved ejection fraction (HFpEF),<sup>1</sup> and rise in extravascular lung water (EVLW) during exercise contributes to symptom occurrence.<sup>2</sup>

Pulmonary congestion is linked to different haemodynamic derangements [elevation in cardiac filling pressures and also higher right atrial (RA) pressures due to impaired right ventricular (RV)–pulmonary artery coupling] as demonstrated in HFpEF patients undergoing invasive haemodynamic testing during submaximal exercise<sup>2</sup>; additionally, a significant

systolic reserve limitation upon exertion (reduced cardiac output/stroke volume) is coupled with elevation of cardiac filling pressures.<sup>3–5</sup>

Stress echocardiography allows assessment of symptoms and dynamic changes of estimated left ventricular (LV) filling pressures during exercise (viz.  $E/e'$  ratio),<sup>6</sup> and it has been recently incorporated into the European consensus recommendation for diagnosis of HFpEF.<sup>7</sup>

Lung ultrasonography (LUS) provides a reliable semi-quantitative evaluation of EVLW in HF patients in different settings.<sup>8–14</sup> Coupled with submaximal exercise stress echocardiography, LUS allows to monitor pulmonary congestion development in HFpEF, which occurs together with dynamic changes of  $E/e'$  and natriuretic peptides.<sup>15</sup> We recently demonstrated that exercise-induced pulmonary congestion as assessed by LUS is an independent predictor of outcomes in patients with HFpEF, and it might allow to further refine risk stratification of these patients on top of well-established prognosticators; B-lines >10 (both as change from rest and as peak value) appeared as the best risk stratifier.<sup>16</sup> Yet changes in cardiac function in patients developing pulmonary congestion on exertion have been scarcely studied.

This study aims at investigating echocardiographic predictors of developed pulmonary congestion as assessed by LUS during exercise stress echocardiography in HFpEF patients.

## Methods

### Participants

Detailed methodology for clinical examination and echocardiographic and statistical methods are reported in the Supporting Information. Consecutive HFpEF outpatients referred to the Cardiology Clinic of the Niška Banja Institute (1 June 2016–1 November 2018) were prospectively enrolled. This cohort expands findings coming from a previous study, which included 61 HFpEF patients and 19 controls.<sup>15,16</sup> Participants, diagnosed according to the European HF guidelines,<sup>17</sup> were haemodynamically stable; exercise stress echocardiography was performed >8 weeks after any previous HF hospitalization. Given the limitations of natriuretic peptide diagnostic thresholds in diagnosing HFpEF,<sup>18</sup> patients having BNP concentrations lower than the 35 pg/mL cut-off proposed by the European HF guidelines<sup>17</sup> were included if they had a previous HF hospitalization. Inclusion criteria were as follows: (i) ability to perform bicycle exercise stress echocardiography, (ii) sinus rhythm, (iii) good echocardiographic window, and (iv) no pulmonary fibrosis or other pulmonary diseases potentially hampering image acquisition (pleural effusion, severe emphysema, previous pneumectomy or lobectomy, pulmonary cancer, or metastases).

The final cohort ( $N = 81$ ) was extracted from the whole population, which was made up of 92 HFpEF patients. Of these, 11 patients did not satisfy the inclusion criteria, seven patients had atrial fibrillation and four patients had severe pulmonary diseases limiting image acquisition. The study was approved by the local ethics committee and managed in accordance with Good Clinical Practice and the Declaration of Helsinki. All patients provided written informed consent. The outcome of interest, a composite of cardiovascular death or HF hospitalization, was ascertained by chart review, institution's electronic medical records, and telephone contact at 1 year. There were no missing data with respect to the study endpoint.

### Submaximal exercise stress echocardiography protocol

After clinical examination, resting echocardiography and LUS were performed (see the succeeding text); patients underwent submaximal exercise stress echocardiography (supine, slightly tilted on their left side) on a tilting table using a cycle ergometer, as proposed by Cardiff-MEDIA protocol (slightly modified to provide a suitable acquisition period to perform both echocardiography and LUS).<sup>19–21</sup> Submaximal exercise stress echocardiography has a good feasibility, allowing image acquisition throughout exercise.<sup>21,22</sup> Exercise started at an initial 15 W workload, with 5 W increments every minute and maintaining a pedalling rate of 55–65 r.p.m. Once heart rate >100 b.p.m. was reached, workload was kept constant for ~5–6 min while echocardiography, LUS imaging, and blood sampling for natriuretic peptides assessment were performed; subsequently, a 10 min recovery phase started. Echocardiography and lung ultrasonography were performed (i) at rest; (ii) during exercise, that is, at the heart rate of >100 b.p.m, or whenever symptoms developed (whichever first); and (iii) during the last 5 min of recovery; electrocardiogram and blood pressure (BP) were continuously monitored and recorded every 2 min throughout the test. For echocardiographic images, at least three consecutive beats were acquired. Exercise testing was interrupted in the event of typical chest pain, constraining breathlessness, dizziness, muscular exhaustion, >10 mmHg drop in systolic BP or severe hypertension (systolic BP  $\geq$  250 mmHg), development of significant ventricular arrhythmias, or ST depression.

### Two-dimensional tissue Doppler echocardiography and lung ultrasonography

Patients underwent detailed echocardiographic examination (Esaote-MyLab Alpha eHD Crystalline Series 7400) using a 1–4 MHz phased-array probe, and lung ultrasonography at

rest and at the maximal workload sustained during exercise (see the Supporting Information for expanded methods). Early filling (E) and atrial (A) peak velocities, and deceleration time of early filling, were measured from transmitral flow. Septal and lateral peak mitral annular early diastolic velocity (*e'*) were acquired and averaged, by real-time pulse-wave tissue Doppler method.<sup>23</sup> LV filling pressures were then estimated by E/*e'* ratio.<sup>23</sup> Tricuspid annular peak systolic excursion (TAPSE) was assessed using M-mode echocardiography. Estimation of pulmonary artery systolic pressure (PASP) was performed using the Bernoulli formula according to tricuspid regurgitation velocity (TRV),<sup>23</sup> as suggested by current recommendations on diastolic stress echocardiography.<sup>21</sup> Assessment of right atrial pressure via vena cava measurements was not performed as it could be challenging during exercise. Three cardiac cycles were obtained from the standard apical long-axis view and four-chamber and two-chamber views. Myocardial longitudinal strain analysis was performed by vector velocity imaging (VVI) using offline software XStrain™. Strain analysis provides accurate estimates of longitudinal deformation.<sup>24–26</sup> VVI quantifies myocardial motion from bi-dimensional clips by automatically tracking operator-defined endocardial and epicardial contours to delineate inward and outward myocardial motion. Longitudinal strain parameters were recorded after confirmation of best wall motion tracking (by operator visual assessment).<sup>27</sup> Then, from LV longitudinal systolic and diastolic strain rate curves for three views, we derived global strain rate (GSR) during systole (GSRs), early diastole (GSR<sub>e</sub>), late diastole (GSR<sub>a</sub>), and isovolumic relaxation period (GSR<sub>ivr</sub>). Global values of strain and strain rate were obtained by averaging the segmental strain values (six segments in each of the three apical views, for a total of 18 segments). We also obtained other two diastolic parameters dividing E-wave by selected strain parameters: (i) E/GSR<sub>e</sub> and (ii) E/GSR<sub>ivr</sub>. We report more negative global longitudinal strain (GLS) and GSR values as 'higher' (defying mathematical logic) because more negative values represent increased myocardial contraction.

Lung ultrasound examinations were performed by the 28-scanning point method<sup>28</sup> immediately after echocardiogram. Scanning sites with missing B-line data (e.g. due to minimal pleural effusions or difficulty in detecting pleural sliding) were judged as 'zero B-lines'.

Echocardiographic images were recorded and analysed offline. The number of B-lines was assessed in real time; additionally, B-line clips were recorded in order to allow offline analysis. The sum of B-lines recorded in each of the 28 scanning points yields a score (ranging from 0 to 280) denoting the extent of extravascular fluid in the lung.<sup>29</sup> All exams were performed by a single operator (D. S.), blinded to patients' data and who did not take part in their clinical management. Typically, 3 min, or less, was necessary to perform echocardiographic acquisitions at peak exercise

(focused on cardiac volumes, PASP, and E/*e'* ratio) or LUS (overall, about 5–6 min for both techniques). Intra-observer and inter-observer variability for strain and strain rate parameters was assessed in 20 randomly selected patients (Supporting Information, *Table S1*). Reliability was excellent, with all coefficients >0.90.

## Laboratory examinations

Immediately before exercise stress echocardiography, peripheral venous blood samples were obtained to determine blood count, sodium, potassium, creatinine (and estimated glomerular filtration rate by modification of diet in renal disease), and BNP; an additional blood sample for BNP was obtained at peak exercise (during echocardiographic image acquisition), just before recovery.<sup>30</sup> BNP concentrations were assessed by Alere™ Triage® BNP MeterPro Assay (Alere San Diego Inc., San Diego, CA, USA).

## Statistical methods

Continuous variables are expressed as mean ± standard deviation, or median and inter-quartile range, as appropriate; categorical variables are presented as counts and percentages. Distribution of variables was visually checked. Differences in baseline characteristics (demographic, clinical, and echocardiographic at rest) and echocardiographic measurements (standard and strain) during exercise (peak exercise, and absolute and per cent change from rest to peak exercise) were assessed according to peak B-lines >10, a cut-off with a well-known prognostic value in HFpEF,<sup>16</sup> and in other setting<sup>31</sup>; furthermore, this reference value approximately corresponds to median and average peak value in our total cohort. Between-group (peak B-line ≤10 vs. peak B-line >10) differences were assessed by unpaired *t*-test or Mann–Whitney test for continuous variables, and  $\chi^2$  test or Fisher's exact test for categorical variables, as appropriate. Within-group measurements at rest vs. peak exercise were compared by paired *t*-test or Wilcoxon signed-rank test, as appropriate. The relationship between peak B-line and standard and strain echocardiographic measurements was assessed by Spearman's correlation coefficient ( $r_s$ ) analysis. Multiple linear regression analysis after adjustment for potential confounders was performed, the dependent variable being peak B-lines and the independent variables being standard and strain echocardiographic measurements. Each echocardiographic parameter (at peak exercise, and absolute and relative changes) was separately assessed to avoid multicollinearity issues. The model used for adjustment in all multivariable analyses included age, sex, coronary artery disease, diabetes, LV mass index, left atrial volume index, and BNP at peak exercise. Additionally, independent

predictors of peak B-lines among clinical and echocardiographic parameters were assessed using multiple linear regression with backward elimination method. Variables identified by previous univariate analysis (with a  $P$ -value  $<0.05$ ) were retained for the final model, along with sex difference and age. Independent predictive value of (i) rest, (ii) peak, and (iii) absolute changes of selected echocardiographic parameters (average  $E/e'$ , GLS, and all GSR parameters) were assessed in separate models, containing all the previously mentioned echocardiographic parameters and other significant baseline predictors by univariate analysis. Tolerance and variance inflation factor were used to check for multicollinearity. Coefficient of multiple determination adjusted for the number of predictors in the model (adjusted  $R^2$ ) was assessed for each model. A  $P$ -value  $<0.05$  was considered significant. Statistical analyses were performed using SPSS package Version 25.0 (Chicago, IL, USA).

## Results

### Clinical and resting echocardiographic characteristics

Main clinical and resting echocardiographic characteristics of the 81 patients enrolled are shown in *Tables 1* and *2*. In the whole population, 43.2% of patients were male, mean age was  $65.0 \pm 8.2$  years, and median LV ejection fraction (LVEF) was 57.2% (inter-quartile range 53.0–62.79). Grouped by exercise LUS findings [39/81 (48.1%) with peak B-lines  $>10$ ; 42/81 (51.9%) with peak B-lines  $\leq 10$ ], patients with peak B-lines  $>10$  were more likely to have coronary artery disease (CAD) or to be on statin, and less likely to have diabetes, compared with patients with B-lines  $\leq 10$ , and higher BNP levels (rest, peak, and absolute difference) (*Table 1*). LV mass index, left atrial volume index, and wall thicknesses were significantly higher in patients with B-lines  $>10$ ; on the other hand,

**Table 1** Baseline demographic and clinical characteristics (whole cohort and according to B-line peak  $>10$  or  $\leq 10$ )

	HFpEF ( $N = 81, 100\%$ )	B-lines $\leq 10$ ( $N = 42, 51.9\%$ )	B-lines $>10$ ( $N = 39, 48.1\%$ )	$P$ -value
<b>Demographics</b>				
Male, $n$ (%)	35 (43.2%)	18 (42.9%)	17 (43.6%)	0.947
Age (years), mean ( $\pm$ SD)	$65.0 \pm 8.2$	$63.9 \pm 8.5$	$66.2 \pm 7.8$	0.209
BMI ( $\text{kg}/\text{m}^2$ ), mean ( $\pm$ SD)	$29.2 \pm 3.6$	$29.5 \pm 3.8$	$28.8 \pm 3.4$	0.388
<b>Medical history</b>				
Hypertension, $n$ (%)	81 (100%)	42 (100%)	39 (100%)	NA
Diabetes, $n$ (%)	28 (34.6%)	20 (47.6%)	8 (20.5%)	0.01
Dyslipidaemia, $n$ (%)	79 (97.5%)	42 (100.0%)	37 (94.9%)	0.137
Coronary artery disease, $n$ (%)	25 (30.9%)	7 (16.7%)	18 (46.2%)	0.004
Current smoking, $n$ (%)	24 (29.6%)	10 (23.8%)	14 (35.9%)	0.234
COPD, $n$ (%)	3 (3.7%)	2 (4.8%)	1 (2.6%)	0.601
Previous HHF, $n$ (%)	70 (86.4%)	35 (83.3%)	35 (89.7%)	0.400
Previous AF episode, $n$ (%)	14 (17.3%)	5 (11.9%)	9 (23.1%)	0.184
NYHA class $>1$	19 (23.5%)	11 (26.2%)	8 (20.5%)	0.547
<b>Therapy</b>				
ACE-i or ARB, $n$ (%)	76 (93.8%)	41 (97.6%)	35 (89.7%)	0.141
Beta-blocker, $n$ (%)	81 (100.0%)	42 (100.0%)	39 (100.0%)	NA
Statin, $n$ (%)	77 (95.1%)	38 (90.5%)	39 (100.0%)	0.048
Diuretics, $n$ (%)	70 (86.4%)	36 (85.7%)	34 (87.2%)	0.847
Nitrates, $n$ (%)	16 (19.8%)	7 (16.7%)	9 (23.1%)	0.469
Aldosterone antagonist, $n$ (%)	14 (17.3%)	4 (9.5%)	10 (25.6%)	0.055
<b>Physical examination—ECG</b>				
Systolic BP, rest (mmHg), mean ( $\pm$ SD)	$125.2 \pm 8.3$	$124.0 \pm 8.3$	$126.5 \pm 8.3$	0.173
Systolic BP, peak (mmHg), mean ( $\pm$ SD)	$147.0 \pm 9.6$	$147.6 \pm 10.7$	$146.3 \pm 8.2$	0.556
Diastolic BP, rest (mmHg), mean ( $\pm$ SD)	$75.0 \pm 7.1$	$74.7 \pm 6.7$	$75.4 \pm 7.5$	0.695
Diastolic BP, peak (mmHg), mean ( $\pm$ SD)	$79.3 \pm 6.0$	$80.5 \pm 6.1$	$78.1 \pm 5.7$	0.066
Heart rate, rest (b.p.m.), mean ( $\pm$ SD)	$64.4 \pm 8.5$	$65.2 \pm 7.1$	$63.6 \pm 9.9$	0.417
Heart rate, peak (b.p.m.), mean ( $\pm$ SD)	$104.0 \pm 6.3$	$103.8 \pm 5.0$	$104.0 \pm 7.5$	0.865
<b>Laboratory</b>				
Haemoglobin (g/dL), mean ( $\pm$ SD)	$13.3 \pm 1.4$	$13.6 \pm 1.9$	$13.0 \pm 15.4$	0.079
Creatinine (mg/dL), mean ( $\pm$ SD)	$1.0 \pm 0.2$	$1.0 \pm 0.2$	$1.0 \pm 0.3$	0.652
Clearance creatinine ( $\text{mL}/\text{min}/1.73$ ), mean ( $\pm$ SD)	$79.0 \pm 21.0$	$81.8 \pm 20.6$	$75.0 \pm 21.0$	0.148
BNP rest (pg/mL), mean ( $\pm$ SD)	$49.3 \pm 41.7$	$29.3 \pm 23.9$	$70.7 \pm 47.1$	$<0.0001$
BNP peak (pg/mL), mean ( $\pm$ SD)	$86.0 \pm 62.4$	$50.8 \pm 28.2$	$124.0 \pm 67.1$	$<0.0001$
BNP change (pg/mL), mean ( $\pm$ SD)	$36.8 \pm 32.3$	$21.4 \pm 15.8$	$53.2 \pm 37.2$	$<0.0001$
BNP change (%)	$123.2 \pm 168.1$	$133.7 \pm 208.5$	$111.8 \pm 111.2$	0.562

ACE-i, angiotensin-converting enzyme inhibitor; AF, atrial fibrillation; ARB, angiotensin II receptor blocker; BMI, body mass index; BNP, B-type natriuretic peptide; BP, blood pressure; COPD, chronic obstructive pulmonary disease; ECG, electrocardiogram; HFpEF, heart failure with preserved ejection fraction; HHF, heart failure hospitalization; NYHA, New York Heart Association; SD, standard deviation.

**Table 2** Standard and strain echocardiographic measurements at rest (whole cohort and according to B-line peak >10 or ≤10)

	HFpEF (N = 81, 100%)	B-lines ≤10 (N = 42, 51.9%)	B-lines >10 (N = 39, 48.1%)	P-value
Diastolic interventricular septum (mm), mean (±SD)	13.8 ± 1.6	13.2 ± 1.2	14.5 ± 1.7	<0.0001
Posterior wall thickness (mm), mean (±SD)	11.6 ± 1.3	11.0 ± 1.1	12.2 ± 1.2	<0.0001
LV diastolic diameter (mm), mean (±SD)	50.1 ± 4.4	50.6 ± 3.8	49.6 ± 5.0	0.302
Relative wall thickness, mean (±SD)	0.47 ± 0.1	0.44 ± 0.1	0.50 ± 0.1	<0.0001
LV mass index (g/m <sup>2</sup> ), mean (±SD)	133.0 ± 28.5	122.1 ± 19.9	144.8 ± 31.8	<0.0001
LV EDV (mL/m <sup>2</sup> ), mean (±SD)	44.0 ± 8.9	43.9 ± 9.5	44.2 ± 8.3	0.847
LV ejection fraction (%), median (IQR)	57.2 (53.0–62.7)	54.6 (51.0–61.1)	57.2 (54.0–63.3)	0.208
Left atrial volume index (mL/m <sup>2</sup> ), mean (±SD)	29.2 ± 7.8	27.2 ± 7.6	30.2 ± 7.1	0.013
E-wave (cm/s), mean (±SD)	56.2 ± 13.9	57.5 ± 15.1	54.7 ± 12.4	0.367
A-wave (cm/s), mean (±SD)	86.9 ± 18.8	86.0 ± 17.8	87.8 ± 19.9	0.670
E/A, mean (±SD)	0.68 ± 0.4	0.68 ± 0.2	0.69 ± 0.5	0.847
Average <i>e'</i> , median (IQR)	7.7 ± 2.1	8.3 ± 2.4	7.1 ± 1.4	0.009
Average E/ <i>e'</i> , median (IQR)	7.8 ± 2.3	7.6 ± 2.5	8.0 ± 1.9	0.438
TAPSE (mm), mean (±SD)	22.2 ± 2.6	22.3 ± 2.4	22.0 ± 2.4	0.262
<i>s'</i> (cm/s), median (IQR)	13.0 (12.0–16.0)	13.5 (12.0–15.3)	13.0 (12.0–18.0)	0.687
TR max velocity—rest (m/s), median (±IQR)	1.8 ± 0.5	1.7 ± 0.5	1.9 ± 0.6	0.308
GLS (%), mean (±SD)	−16.8 ± 1.1	−17.2 ± 1.1	−16.3 ± 0.9	<0.0001
GSRs (1/s), median (IQR)	0.82 (0.76–0.85)	0.83 (0.80–0.85)	0.81 (0.74–0.84)	0.015
GSR <sub>e</sub> (1/s), mean (±SD)	0.94 ± 0.1	0.97 ± 0.1	0.91 ± 0.1	0.016
GSR <sub>a</sub> (1/s), mean (±SD)	0.69 ± 0.1	0.69 ± 0.1	0.69 ± 0.1	0.901
GSR <sub>ivr</sub> (1/s), mean (±SD)	0.43 ± 0.1	0.45 ± 0.1	0.40 ± 0.1	0.002
E-wave/GSR <sub>e</sub> , mean (±SD)	60.9 ± 17.6	60.0 ± 16.8	61.8 ± 18.5	0.662
E-wave/GSR <sub>ivr</sub> , mean (±SD)	137.6 ± 48.5	129.2 ± 36.1	146.6 ± 58.2	0.107
Rest B-lines, median (IQR)	2 (1–4)	1.5 (0–3)	3 (2–4)	<0.0001

EDV, end-diastolic volume; GLS, global longitudinal strain; GSR<sub>a</sub>, global strain rate during late diastole; GSR<sub>e</sub>, global strain rate during early diastole; GSR<sub>ivr</sub>, global strain rate during the isovolumic relaxation; GSRs, systolic global strain rate; HFpEF, heart failure with preserved ejection fraction; IQR, inter-quartile range; LV, left ventricular; SD, standard deviation; TAPSE, tricuspid annular plane systolic excursion; TR, tricuspid regurgitation.

average *e'* and all resting strain and strain rate parameters (except GSR<sub>a</sub>) were lower in that subgroup compared with B-lines ≤10 (Table 2).

B-line reading was interpretable in all patients. At rest, no B-line was present in 15 patients (18.5%). Median rest B-lines were 2 (inter-quartile range 1–4), and patients with peak B-lines >10 displayed higher rest B-lines (Table 2). Overall, exercise test lasted 6.3 ± 1.6 min, and mean achieved workload was 41.0 ± 8.4 W, with no significant difference between peak B-line subgroups. All patients were able to complete the exercise protocol. Changes of systolic and diastolic BP and heart rate upon exercise were significant in whole cohort and in both subgroups (*P* < 0.0001 for all); there were no difference with respect to rest and peak values of BP and heart rate between both subgroups (Table 1).

### Dynamic changes of standard and strain echocardiographic characteristics

Rest and peak values of standard and strain echocardiographic parameters are shown in Supporting Information, Tables S2 and S3. All echocardiographic parameters (except A-wave, and GSR<sub>e</sub> in patients with B-line >10) significantly increased upon exercise in the whole cohort, as well as when patients were subgrouped according to peak B-lines (all *P*-values < 0.002). Peak values (as their absolute and relative changes) of E-wave and its derived indices (E/A, average E/*e'*,

and all derived strain rate ratios) were significantly higher in patients with peak B-lines >10 as opposed to those with peak B-lines ≤10; likewise, the opposite was observed for systolic and diastolic strain rate parameters (Supporting Information, Tables S2 and S3).

### Relationship between B-lines and echocardiographic parameters

Correlation analysis results are displayed in Table 3, showing the relationship between each echocardiographic parameter and peak B-lines. Overall, peak and change values of E-wave, average E/*e'*, GLS, GSRs, GSR<sub>e</sub>, GSR<sub>ivr</sub>, E/GSR<sub>e</sub>, and E/GSR<sub>ivr</sub> showed moderate strength in terms of correlation coefficients, which were statistically significant (all *P*-values < 0.03). Correlation coefficients were weak but also statistically significant for E/A, GSR<sub>a</sub> (change values), and average *e'* (peak value); other echocardiographic parameters (including LVEF) showed weak, non-significant correlation. Among significant parameters, E-wave, its derived indices (i.e. E/A, average E/*e'*, E/GSR<sub>e</sub>, and E/GSR<sub>ivr</sub>), and peak and absolute change of GLS showed positive correlation coefficients; correlation coefficients were negative for all strain rate parameters and relative change of GLS (Table 3). Figure 1 shows dot plot graph for peak and relative change values for two of the most representative parameters of systolic and diastolic function (GLS and average E/*e'*, Panels A and B, respectively).

**Table 3** Correlation analysis and adjusted multiple regression analysis between different echocardiographic parameters (peak, change, and per cent change from baseline) and peak B-lines

	Correlation analysis		Adjusted multiple regression analysis	
	Spearman rho	P-value	Beta coefficient (standard error)	P-values
E-wave (cm/s)	0.47	<0.0001	0.036 (0.013)	0.009
ΔE-wave (cm/s)	0.48	<0.0001	0.040 (0.014)	0.006
(%)ΔE-wave	0.37	0.001	0.013 (0.006)	0.034
E/A	0.22	0.045	0.509 (0.895)	0.571
ΔE/A	0.32	0.004	1.253 (0.726)	0.089
(%)ΔE/A	0.36	0.001	0.011 (0.006)	0.064
Average e'	-0.23	0.038	-0.406 (0.138)	0.004
Δaverage e'	0.01	0.918	0.122 (0.302)	0.689
(%)Δaverage e'	0.10	0.412	0.026 (0.020)	0.203
Average E/e'	0.54	<0.0001	0.309 (0.086)	0.001
Δaverage E/e'	0.41	<0.0001	0.272 (0.109)	0.015
(%)Δaverage E/e'	0.25	0.023	0.013 (0.007)	0.042
LV ejection fraction (%) (IQR)	-0.04	0.737	-0.027 (0.041)	0.521
ΔLV ejection fraction (%), median (IQR)	-0.13	0.256	-0.018 (0.080)	0.824
(%)ΔLV ejection fraction, median (IQR)	-0.13	0.253	-0.011 (0.042)	0.792
GLS (%) <sup>a</sup>	0.47	<0.0001	0.544 (0.249)	0.032
ΔGLS (%)	0.42	<0.0001	0.497 (0.560)	0.377
(%)ΔGLS	-0.39	<0.0001	-0.068 (0.096)	0.482
GSRs (1/s)	-0.38	<0.0001	-1.684 (2.902)	0.563
ΔGSRs (1/s)	-0.41	<0.0001	-6.319 (4.742)	0.187
(%)ΔGSRs (1/s)	-0.44	<0.0001	-0.061 (0.041)	0.141
GSR <sub>e</sub> (1/s)	-0.35	0.002	-1.054 (1.270)	0.409
ΔGSR <sub>e</sub> (1/s)	-0.49	<0.0001	-0.451 (1.413)	0.751
(%)ΔGSR <sub>e</sub>	-0.50	<0.0001	-0.004 (0.014)	0.763
GSR <sub>a</sub> (1/s)	-0.18	0.107	-1.167 (3.615)	0.748
ΔGSR <sub>a</sub> (1/s)	-0.31	0.006	-8.745 (5.936)	0.145
(%)ΔGSR <sub>a</sub>	-0.31	0.005	-0.069 (0.042)	0.106
GSR <sub>iv</sub> (1/s)	-0.43	<0.0001	-9.080 (3.663)	0.016
ΔGSR <sub>iv</sub> (1/s)	-0.39	<0.0001	-21.526 (7.753)	0.007
(%)ΔGSR <sub>iv</sub>	-0.30	0.007	-0.079 (0.035)	0.026
E-wave/GSR <sub>e</sub> (1/s)	0.56	<0.0001	0.002 (0.002)	0.485
ΔE-wave/GSR <sub>e</sub> (1/s)	0.55	<0.0001	0.001 (0.002)	0.534
(%)ΔE-wave/GSR <sub>e</sub> (%)	0.42	<0.0001	0.001 (0.001)	0.641
E-wave/GSR <sub>iv</sub> (1/s)	0.57	<0.0001	0.012 (0.004)	0.003
ΔE-wave/GSR <sub>iv</sub> (1/s)	0.56	<0.0001	0.017 (0.005)	0.001
(%)ΔE-wave/GSR <sub>iv</sub> (1/s)	0.42	<0.0001	0.018 (0.007)	0.007
Rest B-lines	0.47	<0.0001	0.282 (0.228)	0.221

BNP, B-type natriuretic peptide; CAD, coronary artery disease; GLS, global longitudinal strain; GSR<sub>a</sub>, global strain rate during late diastole; GSR<sub>e</sub>, global strain rate during early diastole; GSR<sub>iv</sub>, global strain rate during the isovolumic relaxation; GSRs, systolic global strain rate; IQR, inter-quartile range; LV, left ventricular.

Model for adjustment: age, gender, CAD, diabetes, left ventricular mass index, left atrial volume index, and BNP at peak exercise.

<sup>a</sup>Analyses for GLS were performed with negative values; (%)Δ, per cent variation from baseline.

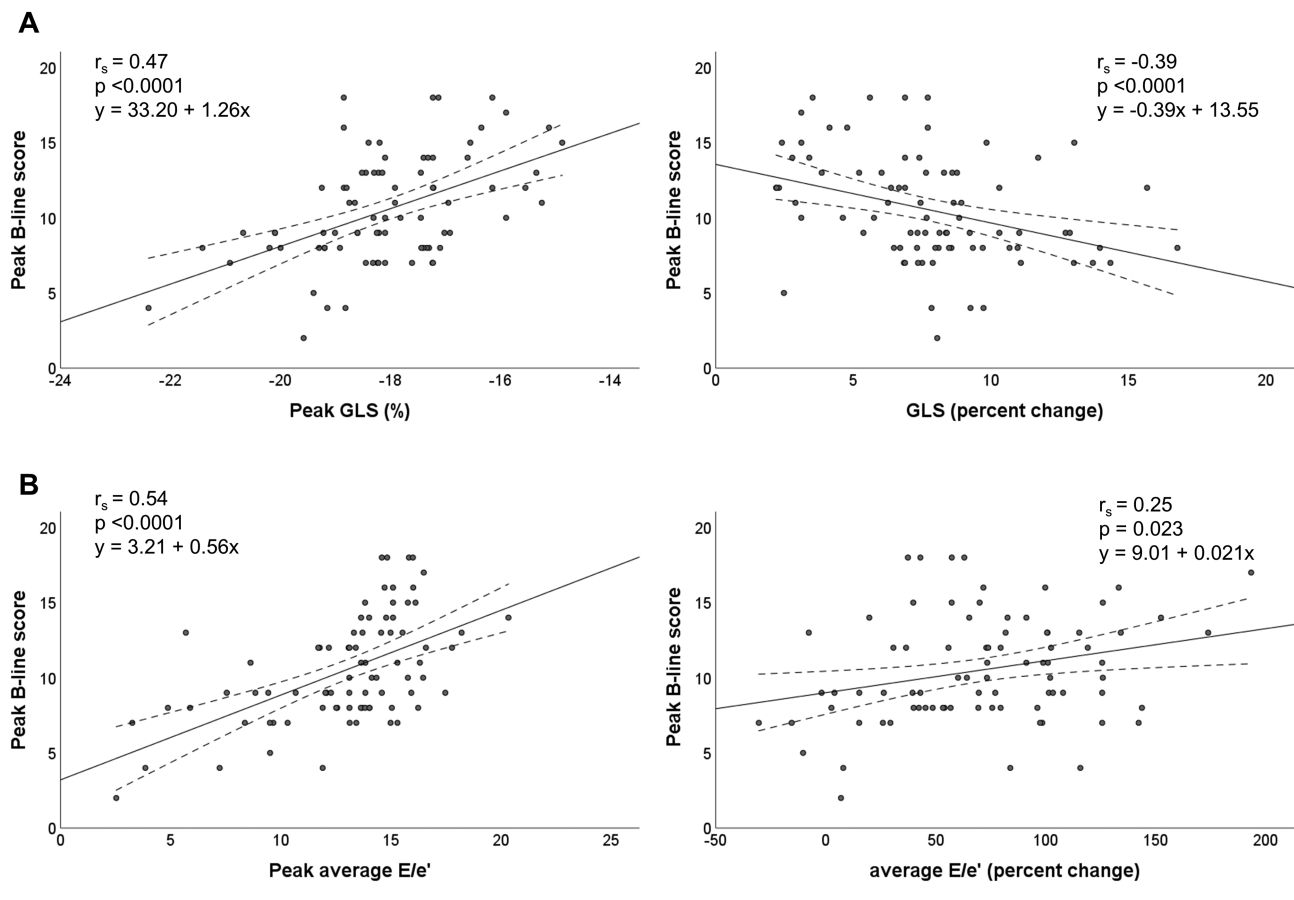
Overall, by adjusted multiple regression analyses, diastolic parameters showed higher association with peak B-lines (Table 3). Specifically, GSR<sub>iv</sub>, E-wave and some of its derived indices (i.e. E/e' and E/GSR<sub>iv</sub>), and peak average e' persisted as significant predictors after model adjustment (all P-values <0.045). Among systolic parameters, peak GLS was significantly associated with peak B-lines (Table 3). No significant associations were found for LVEF.

Figure 2 visually illustrates the interplay of systolic and diastolic function upon exercise in determining peak B-lines. For each tertile of GLS, increasing tertiles of average E/e' were associated with increasing average peak B-lines; the same was observed with increasing GLS tertiles when considering each tertile of average E/e'. There was no significant interaction between the two variables (P for interaction = 0.846).

## Independent predictors of exercise B-lines

Among baseline parameters, history of CAD, diabetes, use of statin, and aldosterone antagonist, rest BNP, rest B-lines, and LV mass index were significantly associated with peak B-lines by univariable analysis (all P-values <0.03) (Table 4). We then built a model including the previously mentioned parameters, age, gender, and resting values of standard and strain parameters. According to the result of multivariable analysis, patients who developed pulmonary congestion upon exercise were characterized by high values of rest BNP, rest B-lines, or LV mass index, with no history of diabetes but with CAD, and by high values of average E/e' and lower values of GSR<sub>iv</sub> (all P-values <0.05). The adjusted R<sup>2</sup> of this model was equal to 0.701.

**Figure 1** Correlations of global longitudinal strain (GLS) (Panel A), and average E/e' (Panel B) with peak B-lines (peak and percent change from baseline).



We then assessed the independent predictive value of peak standard and strain echocardiographic parameters; in addition to diabetes, rest BNP, and rest B-lines, peak values average E/e' and GSRa were retained as independent predictors of peak B-lines ( $P$ -values  $< 0.04$  for both parameters). Adjusted  $R^2$  of this model was 0.776, substantially improving the model fit compared with the model with echocardiographic parameters at rest. Finally, average E/e' and GSRiv were retained as significant predictors by multivariable analysis including absolute changes of echocardiographic parameters, with an adjusted  $R^2$  of 0.740. Similar results were reported when introducing E-wave and average e' in place of average E/e'; namely, peak values of both parameters persisted as independent predictors of peak B-lines along with GSRa.

## Discussion

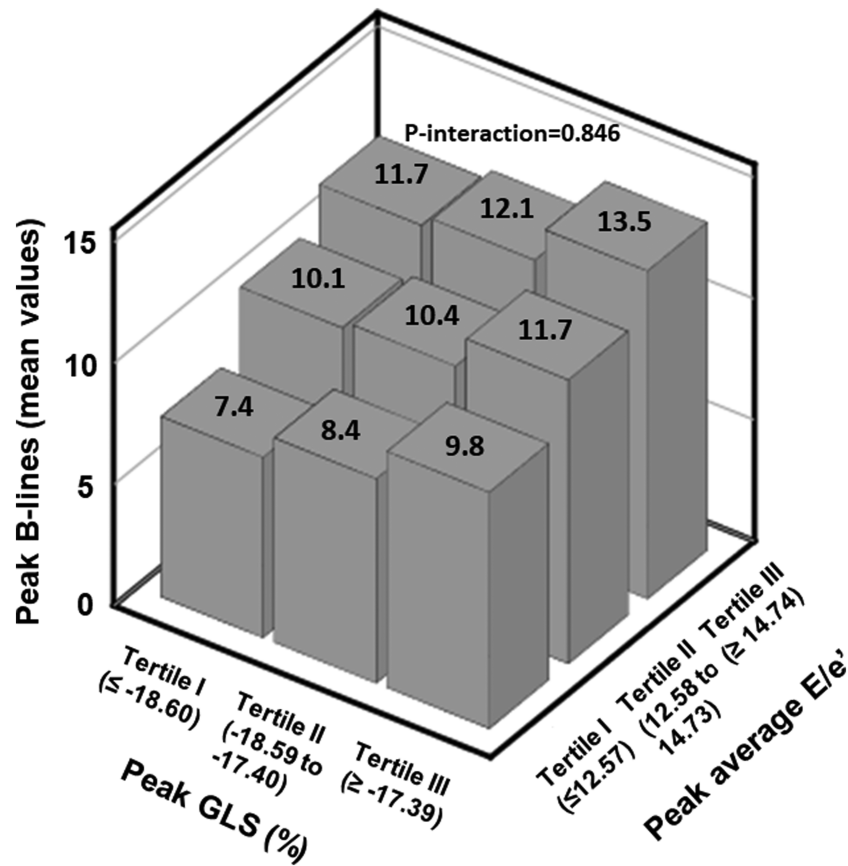
Recent invasive and echocardiographic studies<sup>4,6,15</sup> confirmed that elevation in LV filling pressure during exercise is a hallmark of HFpEF, and this haemodynamic derangement correlates well with severity of exertional dyspnoea.<sup>4</sup> Thus,

development of lung congestion is thought to link symptoms to haemodynamic changes in HFpEF.<sup>3</sup>

Lung ultrasonography is a reliable and reproducible tool to assess EVLW during exercise.<sup>3,15,16,32–34</sup> Recently, we demonstrated that submaximal exercise results in B-line increase in HFpEF patients; those changes were mirrored by significant variations in natriuretic peptides, TRV, and E/e' and were of greater magnitude compared with hypertensive controls.<sup>15</sup> Namely, B-line increases in controls were present but negligible (median B-lines from 0 to 2 during exercise), and overall, exercise B-lines were not significantly correlated with main rest echocardiographic predictors.<sup>15</sup>

Mechanisms underpinning development of B-lines during exercise in HFpEF are not entirely understood, evidence being scarce, mainly deriving from HFREF or mixed cohorts. Agricola *et al.*<sup>34</sup> described B-line kinetics during maximal exercise echocardiography in a mixed cohort of 72 HF patients (average LVEF 41%), with LUS performed in the recovery phase: changes in E/e' and PASP were correlated with B-lines variations. Interestingly, in a small subset with LVEF  $\geq 40\%$  ( $n = 19$ ), which could have included HFpEF patients, change of E/e', but not PASP, was correlated with B-line change<sup>34</sup>; although firm conclusions cannot be drawn because of the



**Figure 2** Average peak B-lines according tertiles of peak values of global longitudinal strain (GLS) and average E/e'.

small sample size, that finding is in line with our results. Overall, we did not find significant subgroup differences (i.e. B-line >10 vs. ≤10) for peak TRV (Supporting Information, Table S2); additionally, correlations between peak B-lines and TRV (peak and absolute change) were, respectively, not significant ( $r_s = 0.12$ ,  $P = 0.29$ ) or weak ( $r_s = 0.31$ ,  $P = 0.006$ ).

In a cohort of 103 HFpEF patients (inclusion LVEF < 45%), Scali *et al.* showed that peak B-lines were tightly correlated with E/e', PASP, and LVEF, with LUS performed at the end of exercise<sup>33</sup>; thus, B-line appearance during exercise in HFpEF seems to be related not only to increases in estimated pulmonary or filling pressures but also to systolic dysfunction as assessed by LVEF. However, LVEF measurement is operator and load dependent, showing limited reproducibility.<sup>35</sup> In order to provide more reliable systolic parameters, we assessed strain and strain rate indices of systolic function (i.e. GLS and GSRs), which are more reproducible and less load dependent compared with LVEF.<sup>36</sup> In our study, patients with B-lines >10 displayed smaller peak values or increase in both GLS and GSRs, compared with patients with B-line ≤10 (Supporting Information, Table S3); in contrast, both subgroups showed similar increments of LVEF upon exercise. Accordingly, by adjusted multiple regression analysis, only peak

GLS and changes of GSRs, but not LVEF, significantly predicted exercise B-lines (Table 3). Thus, reduced contractile reserve seems to partially contribute to development of lung congestion during exercise, also at submaximal workloads, as assessed by strain and strain rate parameters, but LVEF was not sufficiently sensitive to capture those subtle systolic derangements.

On the other hand, although systolic and diastolic function appear to show a certain degree of interdependence in determining exercise B-lines (Figure 2), standard and strain indices of diastolic function showed a tighter association with exercise lung congestion as compared with those of systolic function (Tables 3 and 4); this is not surprisingly considering that diastolic dysfunction and increase in LV filling pressures are the main mechanisms for the development of extravascular lung water during exercise<sup>3</sup> in HFpEF. Namely, average E/e' (and its individual components), GSRa, and GSRiv persisted as independent predictors of exercise B-lines by distinct multivariable analyses including peak or change echocardiographic parameters; conversely, GLS did not (Table 4).

Importantly, among strain parameters, we expanded previous findings on GSRiv, which, at rest, was found to be

Table 4 Univariable and multivariable analysis (backward elimination method) for peak B-lines

	Model with resting echocardiographic predictors			Model with peak echocardiographic predictors			Model with absolute changes of echocardiographic predictors											
	Univariable analysis			Multivariable analysis <sup>a</sup>			Univariable analysis			Multivariable analysis <sup>b</sup>			Univariable analysis			Multivariable analysis <sup>c</sup>		
	Beta coefficient (standard error)	P-value	Beta coefficient (standard error)	P-value	Beta coefficient (standard error)	P-value	Beta coefficient (standard error)	P-value	Beta coefficient (standard error)	P-value	Beta coefficient (standard error)	P-value	Beta coefficient (standard error)	P-value	Beta coefficient (standard error)	P-value		
<b>Baseline significant predictors</b>																		
Male	-0.532 (0.801)	0.508	-0.532 (0.801)	0.508	-0.532 (0.801)	0.508	-0.532 (0.801)	0.508	-0.532 (0.801)	0.508	-0.532 (0.801)	0.508	-0.532 (0.801)	0.508	-0.532 (0.801)	0.508		
Age (years)	0.089 (0.048)	0.068	0.089 (0.048)	0.068	0.089 (0.048)	0.068	0.089 (0.048)	0.068	0.089 (0.048)	0.068	0.089 (0.048)	0.068	0.089 (0.048)	0.068	0.089 (0.048)	0.068		
Diabetes	-2.121 (0.801)	0.01	-2.362 (0.567)	<0.0001	-2.121 (0.801)	0.01	-2.015 (0.496)	<0.0001	-2.121 (0.801)	0.01	-2.015 (0.496)	<0.0001	-2.121 (0.801)	0.01	-1.435 (0.551)	0.009		
Coronary artery disease	1.951 (0.833)	0.022	1.508 (0.570)	0.01	1.951 (0.833)	0.022	1.951 (0.833)	0.022	1.951 (0.833)	0.022	1.951 (0.833)	0.022	1.951 (0.833)	0.022	1.951 (0.833)	0.022		
Statin	5.292 (1.736)	0.003	5.292 (1.736)	0.003	5.292 (1.736)	0.003	5.292 (1.736)	0.003	5.292 (1.736)	0.003	5.292 (1.736)	0.003	5.292 (1.736)	0.003	5.292 (1.736)	0.003		
Aldosterone antagonist	2.294 (1.020)	0.027	2.294 (1.020)	0.027	2.294 (1.020)	0.027	2.294 (1.020)	0.027	2.294 (1.020)	0.027	2.294 (1.020)	0.027	2.294 (1.020)	0.027	2.294 (1.020)	0.027		
BNP rest (pg/mL)	0.049 (0.008)	<0.0001	0.017 (0.009)	0.048	0.049 (0.008)	<0.0001	0.02 (0.007)	0.009	0.049 (0.008)	<0.0001	0.02 (0.007)	0.009	0.049 (0.008)	<0.0001	0.028 (0.008)	0.001		
LV mass index (g/m <sup>2</sup> )	0.049 (0.013)	<0.0001	0.028 (0.009)	0.005	0.049 (0.013)	<0.0001	0.049 (0.013)	<0.0001	0.049 (0.013)	<0.0001	0.049 (0.013)	<0.0001	0.049 (0.013)	<0.0001	0.049 (0.013)	<0.0001		
Rest B-lines	1.109 (0.231)	<0.0001	0.605 (0.221)	0.008	1.109 (0.231)	<0.0001	0.856 (0.198)	<0.0001	1.109 (0.231)	<0.0001	0.856 (0.198)	<0.0001	1.109 (0.231)	<0.0001	0.614 (0.220)	0.007		
<b>Standard and strain echocardiographic predictors</b>																		
Average E/e'	0.459 (0.169)	0.008	0.305 (0.124)	0.016	0.459 (0.169)	0.008	0.461 (0.071)	<0.0001	0.459 (0.169)	0.008	0.461 (0.071)	<0.0001	0.459 (0.169)	0.008	0.358 (0.103)	0.001		
GLS (%)	1.403 (0.325)	<0.0001	1.255 (0.245)	<0.0001	1.403 (0.325)	<0.0001	1.255 (0.245)	<0.0001	1.403 (0.325)	<0.0001	1.255 (0.245)	<0.0001	1.403 (0.325)	<0.0001	0.740			
GSRs (1/s)	-16.336 (5.567)	0.004	-12.957 (3.061)	<0.0001	-16.336 (5.567)	0.004	-12.957 (3.061)	<0.0001	-16.336 (5.567)	0.004	-12.957 (3.061)	<0.0001	-16.336 (5.567)	0.004	-24.005 (5.435)	<0.0001		
GSRs (1/s)	-11.311 (3.550)	0.002	-4.566 (1.597)	0.005	-11.311 (3.550)	0.002	-4.566 (1.597)	0.005	-11.311 (3.550)	0.002	-4.566 (1.597)	0.005	-11.311 (3.550)	0.002	-3.373 (1.982)	0.093		
GSRa (1/s)	-4.982 (5.878)	0.399	-11.122 (4.734)	0.021	-4.982 (5.878)	0.399	-11.122 (4.734)	0.021	-4.982 (5.878)	0.399	-11.122 (4.734)	0.021	-4.982 (5.878)	0.399	-21.282 (7.783)	0.008		
GSRiv (1/s)	-20.481 (5.043)	<0.0001	-10.768 (4.254)	0.014	-20.481 (5.043)	<0.0001	-10.768 (4.254)	0.014	-20.481 (5.043)	<0.0001	-10.768 (4.254)	0.014	-20.481 (5.043)	<0.0001	-19.817 (10.037)	0.001		
Model adjusted R <sup>2</sup>			0.701		0.776		0.776		0.701		0.776		0.776		0.740			

BNP, B-type natriuretic peptide; GLS, global longitudinal strain; GSRa, global strain rate during late diastole; GSRb, global strain rate during early diastole; GSRiv, global strain rate during the isovolumic relaxation; GSRs, systolic global strain rate; LV, left ventricular.

<sup>a</sup>GSRs and GSRb were excluded from the multivariable model because of multicollinearity issues.

<sup>b</sup>GSRs and GSRiv were excluded from the multivariable model because of multicollinearity issues.

<sup>c</sup>GSRs was excluded from the multivariable model because of multicollinearity issues.

independently associated with invasively assessed LV end-diastolic pressures in HFpEF patients.<sup>37</sup> GSRiv also outperformed GSRe and GSRs, which were not retained as significant predictors of LV filling pressures, in line with our results. Indeed, in our study, peak values of both GSRiv and GSRe were significant predictors by univariable analysis (Table 4); however, after model adjustment (which included left atrial volume and BNP), GSRiv showed significant associations with peak B-lines, while GSRe did not (Table 3). GSRiv reflects changes occurring during isovolumic relaxation (i.e. before mitral valve opening) and therefore is less load dependent, better reflecting intrinsic myocardial characteristics of the LV during early LV expansion; on the other hand, GSRe, occurring during early diastole, appears to be mainly influenced by LV wall stress and left atrial pressure.<sup>38</sup>

Recently, in a cohort of 61 HFpEF undergoing invasive haemodynamic exercise testing, B-line appearance or increase (as assessed in 2 points on the left third intercostal space along the mid-axillary and mid-clavicular lines) during submaximal exercise was related to rise in both PCWP and RA pressure and to impairment in RV-to-pulmonary circulation coupling (as assessed by respective ratios of TAPSE or RV  $s'$  and invasive mean pulmonary arterial pressure).<sup>2</sup> The association of RV function with pulmonary congestion has also been reported in patients with worsening HF.<sup>14</sup> In our cohort, rest or peak values of RV  $s'$ , TAPSE, and their respective ratios with TRV were not significantly correlated or associated by linear regression with peak B-lines (data not shown). Differences in terms of baseline characteristics between the two studies are relevant; indeed, Reddy's cohort seems to represent a higher-risk HFpEF population compared with our cohort, illustrated by less severe congestion (average E/e' ratio 8 vs. 12) and better RV systolic function (average RV  $s'$  13 vs. 10 cm/s; average TAPSE 22 vs. 18 mm). Also, we included patients with better functional class (76.5% in NYHA I functional class vs. 'lifestyle-limiting symptoms') and lower average body mass index (29 vs. 34 kg/m<sup>2</sup>). According to HFpEF phenotype classification proposed by Shah,<sup>39</sup> our cohort may represent 'phenotype A', that is, the most frequently seen in HFpEF patients, likely reflecting an earlier stage with few symptoms at rest, initial diastolic dysfunction, preserved RV function, and no pulmonary hypertension at rest. It might be hypothesized that during early stage of HFpEF syndrome, RV-to-pulmonary circulation coupling derangements are less relevant, or contribute little, to exercise-induced lung congestion as compared with their role in increasing PCWP in more advanced disease. However, taking into account differences between our study and that of Reddy *et al.* in terms of exercise protocol (workload achieved 41 vs. 20 W), and methods of pulmonary pressure (estimated vs. invasively measured) and B-line assessment, a direct comparison cannot be made. Indeed, the study of Reddy *et al.*, although more accurate

and reliable with respect to direct pressure measurements, provided B-line assessment obtained from only 2 scanning points (as compared with 28 scanning points in the present study), allowing only a qualitative evaluation (i.e. exercise EVLW yes or not). Additionally, RA pressures were not estimated in our study and thus not taken into account for PASP estimation by TRV; this may have resulted in underestimating non-invasive PASP. Whether differences of HFpEF phenotypes reflect feasibility and accuracy problems—as recently suggested<sup>6</sup>—different timings of PASP rise during exercise, or intrinsic limitations of this parameter (TRV being an indirect estimate of LV filling pressures), is not completely understood.

Pugliese *et al.* recently confirmed the prognostic value of LUS as part of a multi-parametric score in a mixed cohort of 274 patients with HFpEF or at risk of developing HF ( $N = 113$  with Stages A and B and  $N = 161$  with Stage C HFpEF according to American College of Cardiology/American Heart Association Heart Failure Classification,<sup>40</sup> respectively) undergoing symptom-limited cardiopulmonary exercise testing—exercise stress echocardiography.<sup>41</sup> By multivariable Cox proportional hazards models, B-line change  $>10$  (from rest to peak) was retained as an independent predictor of cardiovascular death or HF hospitalization, along with peak oxygen consumption  $<16$  mL/kg/min, minute ventilation/carbon dioxide production slope  $>36$ , PASP  $> 50$  mmHg, and resting N-terminal pro B-type natriuretic peptide  $>900$  pg/mL.<sup>41</sup> A weighted risk score including those predictors (ranging from 0 to 9) accurately predicted adverse events during a median follow-up of 18.5 months. Among those predictors, B-line change  $>10$  showed the tightest association with the combined endpoint (hazard ratio = 7.81, 95% confidence interval 2.62–23.33,  $P < 0.001$ ); this is substantially in line with results of our previous study performed in this cohort<sup>16</sup> (hazard ratio = 4.97, 95% confidence interval 2.08–11.90,  $P < 0.001$ ), although substantial differences in terms exercise protocol (maximal vs. submaximal exercise stress), HFpEF population (American College of Cardiology/American Heart Association Stages A–C vs. I–II NYHA class HFpEF), and LUS methodology (8 scanning zones vs. 28 scanning points) are present. An integrated and more complex assessment with combined cardiopulmonary exercise testing—exercise stress echocardiography can represent a new multi-parametric approach able to further refine prognosis of HFpEF patients and to predict the progression to clinically overt HF of patients at risk for developing this complex syndrome. These findings should be further replicated in larger HFpEF cohorts to prompt the implementation of this multimodality technique.

The present study expands our previous findings on the prognostic value of exercise LUS,<sup>16</sup> which was found to represent a useful prognostic tool in different HF phenotypes.<sup>16,32,33</sup> We have herein demonstrated mechanisms underlying B-line development during exercise, which appears to be mostly related to diastolic function worsening as assessed by echocardiography.

## Limitations

This is a single-centre cohort study, which may limit generalizability of our results; unknown or unmeasured confounding variables that were not adjusted for could have affected the observed relationships. Patients with atrial fibrillation were excluded because of limitations in the evaluation of diastolic function,<sup>23</sup> and this might limit the generalizability of our results. Detection of B-lines does not necessarily imply their cardiogenic origin; however, we excluded patients with pulmonary fibrosis (a disease associated with 'dry' B-lines); furthermore, that phenomenon could have affected basal B-line pattern, but it cannot explain changes in B-lines induced by exercise. Additionally, real-time analysis by a single operator may represent a potential source of bias, although it represents the closest approach to routine clinical practice.

## Conclusions

In HFpEF outpatients, diastolic echocardiographic parameters (standard and strain) appear to be better associated with, and partly explain, the occurrence of exercise-induced pulmonary congestion as assessed by LUS.

## Conflict of interest

N.G. reports personal fees from Novartis, Boehringer, AstraZeneca, Bayer, and Vifor outside the submitted work. G.A. reports personal fees from Angelini, Behring, Menarini, and Novartis outside the submitted work. All the other authors have nothing to declare.

## References

- Roh J, Houstis N, Rosenzweig A. Why don't we have proven treatments for hfpef? *Circ Res.* 2017; **120**: 1243–1245.
- Reddy YNV, Obokata M, Wiley B, Koeppe KE, Jorgenson CC, Egbe A, Melenovsky V, Carter RE, Borlaug BA. The haemodynamic basis of lung congestion during exercise in heart failure with preserved ejection fraction. *Eur Heart J.* 2019; **40**: 3721–3730.
- Borlaug BA, Kane GC, Melenovsky V, Olson TP. Abnormal right ventricular-pulmonary artery coupling with exercise in heart failure with preserved ejection fraction. *Eur Heart J.* 2016; **37**: 3293–3302.
- Obokata M, Olson TP, Reddy YNV, Melenovsky V, Kane GC, Borlaug BA. Haemodynamics, dyspnoea, and pulmonary reserve in heart failure with preserved ejection fraction. *European Heart Journal.* 2018; **39**: 2810–2821.
- Eisman AS, Shah RV, Dhakal BP, Pappagianopoulos PP, Wooster L, Bailey C, Cunningham TF, Hardin KM, Baggish AL, Ho JE, Malhotra R, Lewis GD. Pulmonary capillary wedge pressure patterns during exercise predict exercise capacity and incident heart failure. *Circ Heart Fail.* 2018; **11**: e004750.
- Obokata M, Kane GC, Reddy YNV, Olson TP, Melenovsky V, Borlaug BA. Role of diastolic stress testing in the evaluation for heart failure with preserved ejection fraction. *Circulation.* 2017; **135**: 825–838.
- Pieske B, Tschöpe C, de Boer RA, Fraser AG, Anker SD, Donal E, Edelmann F, Fu M, Guazzi M, Lam CSP, Lancellotti P, Melenovsky V, Morris DA, Nagel E, Pieske-Kraigher E, Ponikowski P, Solomon SD, Vasan RS, Rutten FH, Voors AA, Ruschitzka F, Paulus WJ, Seferovic P, Filippatos G. How to diagnose heart failure with preserved ejection fraction: the hfa-peff diagnostic algorithm: a consensus recommendation from the heart failure association (HFA) of the European Society of Cardiology (ESC). *Eur Heart J* 2019; **40**: 3297–3317.
- Buessler A, Chouihed T, Duarte K, Bassand A, Huot-Marchand M, Gottwalles Y, Penine A, Andre E, Nace L, Jaeger D, Kobayashi M, Coiro S, Rossignol P, Girerd N. Accuracy of several lung ultrasound methods for the diagnosis of acute heart failure in the ed: a multicenter prospective study. *Chest* 2020; **157**: 99–110.

## Funding

This manuscript was partially funded by Programmadi Rete NET-2016-02363853: "Performance evaluation and value assessment for cardiovascular and oncological care paths in a regional network context: challenges and opportunities".

## Author contributions

All authors declare that they have made substantial contributions to all of the following: (i) the conception and design of the study, or acquisition of data, or analysis and interpretation of data; (ii) drafting the article or revising it critically for important intellectual content; and (iii) final approval of the version to be submitted. G.A. is a visiting professor at the University of Niš School of Medicine, Niš, Serbia.

## Supporting information

Additional supporting information may be found online in the Supporting Information section at the end of the article.

**Table S1.** Intra- and inter-observer correlation coefficients of strain parameters.

**Table S2.** Standard echocardiographic measurements at rest and during exercise (whole cohort and according to B-line peak >10 or ≤10).

**Table S3.** Strain echocardiographic measurements at rest and during exercise (whole cohort and according to B-line peak >10 or ≤10).

9. Mottola C, Girerd N, Coiro S, Lamiral Z, Rossignol P, Frimat L, Girerd S. Evaluation of subclinical fluid overload using lung ultrasound and estimated plasma volume in the postoperative period following kidney transplantation. *Transplant Proc* 2018; **50**: 1336–1341.
10. Coiro S, Porot G, Rossignol P, Ambrosio G, Carluccio E, Tritto I, Huttin O, Lemoine S, Sadoul N, Donal E, Zannad F, Girerd N. Prognostic value of pulmonary congestion assessed by lung ultrasound imaging during heart failure hospitalisation: A two-centre cohort study. *Sci Rep*. 2016; **6**: 39426.
11. Chouihed T, Coiro S, Zannad F, Girerd N. Lung ultrasound: a diagnostic and prognostic tool at every step in the pathway of care for acute heart failure. *Am J Emerg Med* 2016; **34**: 656–657.
12. Coiro S, Chouihed T, Girerd N. Lung ultrasound—the extension of clinical examination in patients with acute heart failure: reply. *Eur J Heart Fail* 2016; **18**: 215.
13. Coiro S, Rossignol P, Ambrosio G, Carluccio E, Alunni G, Murrone A, Tritto I, Zannad F, Girerd N. Prognostic value of residual pulmonary congestion at discharge assessed by lung ultrasound imaging in heart failure. *Eur J Heart Fail*. 2015; **17**: 1172–1181.
14. Kobayashi M, Gargani L, Palazzuoli A, Ambrosio G, Bayes-Genis A, Lupon J, Pellicori P, Pugliese NR, Reddy YNV, Ruocco G, Duarte K, Huttin O, Rossignol P, Coiro S, Girerd N. Association between right-sided cardiac function and ultrasound-based pulmonary congestion on acutely decompensated heart failure: Findings from a pooled analysis of four cohort studies. *Clin Res Cardiol*. 2020; **110**: 1181–1192.
15. Simonovic D, Coiro S, Carluccio E, Girerd N, Deljanin-Ilic M, Cattadori G, Ambrosio G. Exercise elicits dynamic changes in extravascular lung water and haemodynamic congestion in heart failure patients with preserved ejection fraction. *Eur J Heart Fail*. 2018; **20**: 1366–1369.
16. Coiro S, Simonovic D, Deljanin-Ilic M, Duarte K, Carluccio E, Cattadori G, Girerd N, Ambrosio G. Prognostic value of dynamic changes in pulmonary congestion during exercise stress echocardiography in heart failure with preserved ejection fraction. *Circ Heart Fail*. 2020; **13**: e006769
17. Ponikowski P, Voors AA, Anker SD, Bueno H, Cleland JG, Coats AJ, Falk V, Gonzalez-Juanatey JR, Harjola VP, Jankowska EA, Jessup M, Linde C, Nihoyannopoulos P, Parissis JT, Pieske B, Riley JP, Rosano GM, Ruitlope LM, Ruschitzka F, Rutten FH, van der Meer P, Authors/Task Force M, Document R. 2016 ESC guidelines for the diagnosis and treatment of acute and chronic heart failure: The task force for the diagnosis and treatment of acute and chronic heart failure of the European society of cardiology (ESC). Developed with the special contribution of the heart failure association (hfa) of the ESC. *Eur J Heart Fail*. 2016; **18**: 891–975.
18. Tanase DM, Radu S, Al Shurbaji S, Baroi GL, Florida Costea C, Turliuc MD, Ouatu A, Floria M. Natriuretic peptides in heart failure with preserved left ventricular ejection fraction: From molecular evidences to clinical implications. *Int J Mol Sci*. 2019; **20**: 2629.
19. Sanchez-Martinez S, Duchateau N, Erdei T, Kunszt G, Aakhus S, Degiovanni A, Marino P, Carluccio E, Piella G, Fraser AG, Bijmens BH. Machine learning analysis of left ventricular function to characterize heart failure with preserved ejection fraction. *Circ Cardiovasc Imaging*. 2018; **11**: e007138.
20. Erdei T, Smiseth OA, Marino P, Fraser AG. A systematic review of diastolic stress tests in heart failure with preserved ejection fraction, with proposals from the eu-fp7 media study group. *Eur J Heart Fail*. 2014; **16**: 1345–1361.
21. Prasad SB, Holland DJ, Atherton JJ. Diastolic stress echocardiography: From basic principles to clinical applications. *Heart*. 2018; **104**: 1739–1748.
22. Donal E, Thebault C, Lund LH, Kervio G, Reynaud A, Simon T, Drouet E, Nonotte E, Linde C, Daubert JC. Heart failure with a preserved ejection fraction additive value of an exercise stress echocardiography. *Eur Heart J Cardiovasc Imaging*. 2012; **13**: 656–665.
23. Nagueh SF, Smiseth OA, Appleton CP, Byrd BF 3rd, Dokainish H, Edvardsen T, Flachskampf FA, Gillebert TC, Klein AL, Lancellotti P, Marino P, Oh JK, Alexandru Popescu B, Waggoner AD. Recommendations for the evaluation of left ventricular diastolic function by echocardiography: An update from the American society of echocardiography and the European association of cardiovascular imaging. *Eur Heart J Cardiovasc Imaging*. 2016; **17**: 1321–1360.
24. Coiro S, Huttin O, Bozec E, Selton-Suty C, Lamiral Z, Carluccio E, Trinh A, Fraser AG, Ambrosio G, Rossignol P, Zannad F, Girerd N. Reproducibility of echocardiographic assessment of 2d-derived longitudinal strain parameters in a population-based study (the stanislas cohort study). *Int J Cardiovasc Imaging*. 2017; **33**: 1361–1369.
25. Huttin O, Girerd N, Coiro S, Bozec E, Selton-Suty C, Lamiral Z, Frikha Z, Kobayashi M, Argulian E, Narula J, Fraser AG, Rossignol P, Zannad F. Association between layer-specific longitudinal strain and risk factors of heart failure and dyspnea: A population-based study. *J Am Soc Echocardiogr*. 2019; **32**: 854–865. e858.
26. Verdugo-Marchese M, Coiro S, Selton-Suty C, Kobayashi M, Bozec E, Lamiral Z, Venner C, Zannad F, Rossignol P, Girerd N, Huttin O. Left ventricular myocardial deformation pattern, mechanical dispersion, and their relation with electrocardiogram markers in the large population-based stanislas cohort: Insights into electromechanical coupling. *European heart journal cardiovascular imaging*. 2020; **21**: 1237–1245.
27. Badran HM, Faheem N, Soliman M, Hamdy M, Yacoub M. Comparison of vector velocity imaging and three-dimensional speckle tracking echocardiography for assessment of left ventricular longitudinal strain in hypertrophic cardiomyopathy. *Glob Cardiol Sci Pract*. 2019; **2019**: 6–6.
28. Jambrik Z, Monti S, Coppola V, Agricola E, Mottola G, Miniati M, Picano E. Usefulness of ultrasound lung comets as a nonradiologic sign of extravascular lung water. *Am J Cardiol*. 2004; **93**: 1265–1270.
29. Volpicelli G, Elbarbary M, Blaivas M, Lichtenstein DA, Mathis G, Kirkpatrick AW, Melniker L, Gargani L, Noble VE, Via G, Dean A, Tsung JW, Soldati G, Copetti R, Bouhemad B, Reissig A, Agricola E, Rouby JJ, Arbelot C, Liteplo A, Sargsyan A, Silva F, Hoppmann R, Breikreutz R, Seibel A, Neri L, Storti E, Petrovic T, International Liaison Committee on Lung Ultrasound for International Consensus Conference on Lung U. International evidence-based recommendations for point-of-care lung ultrasound. *Intensive Care Med*. 2012; **38**: 577–591.
30. Capoulade R, Magne J, Dulgheru R, Hachicha Z, Dumesnil JG, O'Connor K, Arsenault M, Bergeron S, Pierard LA, Lancellotti P, Pibarot P. Prognostic value of plasma b-type natriuretic peptide levels after exercise in patients with severe asymptomatic aortic stenosis. *Heart*. 2014; **100**: 1606–1612.
31. Scali MC, Zagatina A, Ciampi Q, Cortigiani L, D'Andrea A, Daros CB, Zhuravskaya N, Kasprzak JD, Wierzbowska-Drabik K, Luis de Castro ESPJ, Djordjevic-Dikic A, Beleslin B, Petrovic M, Boskovic N, Tesic M, Monte I, Simova I, Vladova M, Boshchenko A, Vrublevsky A, Citro R, Amor M, Vargas Miele PE, Arbucci R, Merlo PM, Lowenstein Haber DM, Dodi C, Rigo F, Gligorova S, Dekleva M, Severino S, Lattanzi F, Morrone D, Galderisi M, Torres MAR, Salustri A, Rodriguez-Zanella H, Costantino FM, Varga A, Agoston G, Bossone E, Ferrara F, Gaibazzi N, Celutkiene J, Haberka M, Mori F, D'Alfonso MG, Reichenhofer B, Camarozano AC, Miglioranza MH, Szymczyk E, Wejner-Mik P, Wdowiak-Okrojek K, Preradovic-Kovacevic T, Bombardini T, Ostojic M, Nikolic A, Re F, Barbieri A, Di Salvo G, Merli E, Colonna P, Lorenzoni V, De Nes M, Paterni M, Carpeggiani C, Lowenstein J, Picano E, Stress Echo Study Group of the Italian Society of E, Cardiovascular I. Lung ultrasound and pulmonary congestion during stress echocardiography. *JACC Cardiovasc Imaging*. 2020; **13**: 2085–2095.

32. Fabiani I, Pugliese NR, Galeotti GG, D'Agostino A, Mazzola M, Pedrinelli R, Dini FL. The added value of exercise stress echocardiography in patients with heart failure. *Am J Cardiol.* 2019; **123**: 1470–1477.
33. Scali MC, Cortigiani L, Simionuc A, Gregori D, Marzilli M, Picano E. Exercise-induced b-lines identify worse functional and prognostic stage in heart failure patients with depressed left ventricular ejection fraction. *Eur J Heart Fail.* 2017; **19**: 1468–1478.
34. Agricola E, Picano E, Oppizzi M, Pisani M, Meris A, Fragasso G, Margonato A. Assessment of stress-induced pulmonary interstitial edema by chest ultrasound during exercise echocardiography and its correlation with left ventricular function. *J Am Soc Echocardiogr.* 2006; **19**: 457–463.
35. Lang RM, Badano LP, Mor-Avi V, Afilalo J, Armstrong A, Ernande L, Flachskampf FA, Foster E, Goldstein SA, Kuznetsova T, Lancellotti P, Muraru D, Picard MH, Rietzschel ER, Rudski L, Spencer KT, Tsang W, Voigt JU. Recommendations for cardiac chamber quantification by echocardiography in adults: An update from the american society of echocardiography and the european association of cardiovascular imaging. *J Am Soc Echocardiogr.* 2015; **28**: 1–39.e14.
36. Negishi K, Borowski AG, Popovic ZB, Greenberg NL, Martin DS, Bungo MW, Levine BD, Thomas JD. Effect of gravitational gradients on cardiac filling and performance. *J Am Soc Echocardiogr.* 2017; **30**: 1180–1188.
37. Hatipoglu S, Özdemir N, Babür Güler G, Bakal RB, Geçmen C, Candan Ö, Dogan C, Unkun T. Prediction of elevated left ventricular filling pressures in patients with preserved ejection fraction using longitudinal deformation indices of the left ventricle. *Eur Heart J Cardiovasc Imaging.* 2015; **16**: 1154–1161.
38. Mor-Avi V, Lang RM, Badano LP, Belohlavek M, Cardim NM, Derumeaux G, Galderisi M, Marwick T, Nagueh SF, Sengupta PP, Sicari R, Smiseth OA, Smulevitz B, Takeuchi M, Thomas JD, Vannan M, Voigt J-U, Zamorano JL. Current and evolving echocardiographic techniques for the quantitative evaluation of cardiac mechanics: ASE/EAE consensus statement on methodology and indications: Endorsed by the Japanese society of echocardiography. *J Am Soc Echocardiogr.* 2011; **24**: 277–313.
39. Shah SJ. Matchmaking for the optimization of clinical trials of heart failure with preserved ejection fraction: No laughing matter. *J Am Coll Cardiol.* 2013; **62**: 1339–1342.
40. Yancy CW, Jessup M, Bozkurt B, Butler J, Casey DE Jr, Drazner MH, Fonarow GC, Geraci SA, Horwich T, Januzzi JL, Johnson MR, Kasper EK, Levy WC, Masoudi FA, McBride PE, McMurray JJ, Mitchell JE, Peterson PN, Riegel B, Sam F, Stevenson LW, Tang WH, Tsai EJ, Wilkoff BL, American College of Cardiology F, American Heart Association Task Force on Practice G. 2013 ACCF/AHA guideline for the management of heart failure: A report of the American college of cardiology foundation/American heart association task force on practice guidelines. *J Am Coll Cardiol.* 2013; **62**: e147–e239.
41. Pugliese NR, de Biase N, Gargani L, Mazzola M, Conte L, Fabiani I, Natali A, Dini FL, Frumento P, Rosada J, Taddei S, Borlaug BA, Masi S. Predicting the transition to and progression of heart failure with preserved ejection fraction: A weighted risk score using biohumoural, cardiopulmonary, and echocardiographic stress testing. *Eur. J Prev Cardiol.* 2020.